Available online at www.sciencedirect.com
SCIENCE DIRECT®
PERGAMON
Solid State Communications 128 (2003) 51–56
solid state communications
www.elsevier.com/locate/ssc

Imaging the structure of the interface between symmetries interconnected by a discontinuous transition

Yanina Fasano, M. De Seta[1], M. Menghini, H. Pastoriza*, F. de la Cruz

Low Temperatures Laboratory, Centro Atómico Bariloche and Instituto Balseiro, CNEA, Av. Bustillo 9500, R8402AGP Bariloche, RN, Argentina

Received 7 July 2003; received in revised form 15 July 2003; accepted 18 July 2003 by M. Cardona

Abstract

We have been able to observe with single particle resolution the interface between two structural symmetries that cannot be interconnected by a continuous transition. By means of an engineered 2D potential that pins the extremity of vortex strings a square symmetry was imposed at the surface of a 3D vortex solid. Using the Bitter decoration technique and on account of the continuous vortex symmetry, we visualize how the induced structure transforms along the vortex direction before changing into the expected hexagonal structure at a finite distance from the surface.

PACS: 74.25.Qt; 74.72.Hs; 64.70.Kb

Keywords: A. Superconductors; B. Nanofabrications; D. Flux pinning and creep

First order phase transitions [1,2] are often associated with a discontinuous change of topological symmetry. The analysis and detection at microscopic scale of mechanisms that allow the nucleation and propagation of new symmetries is a formidable task of difficult experimental resolution. An ensemble of superconducting vortices, having a continuous symmetry along the average vortex orientation and discrete structural symmetry in planes perpendicular to it, is a unique toy model to investigate first and second order phase transitions [3–9].

The vortex liquid in superconducting $Bi_2Sr_2CaCu_2O_8$ crystals transforms through a first order thermodynamic transition into a solid (Bragg Glass [10]) with hexagonal quasi-long range order. As a result of the almost ideal behavior of the vortex structure large vortex single crystals are usually obtained after the liquid–solid transition. The topology of the solid state with individual vortex resolution can be detected by magnetic decoration, observing the clumps generated by small Fe particles deposited at the vortex positions.

The scope of this work is to develop a strategy to investigate how a change of structural symmetry induced at the surface of a solid of elastic strings propagates along their length. This is achieved imposing the vortex liquid to solidify in a three dimensional square lattice at one surface of a $Bi_2Sr_2CaCu_2O_8$ crystal while the natural hexagonal vortex structure is observed at the opposite surface. In this way, we were able to study the vortex structure within the interface between two single crystals of vortices with symmetries that cannot be interconnected by a continuous phase transition.

By means of electron beam lithography Fe dots of 260 nm in diameter and 60 nm height were deposited on the top surface of $Bi_2Sr_2CaCu_2O_8$ single crystals of approximate dimensions $0.5 \times 0.5 \times 0.03$ mm^3. The dots are of similar dimensions as the clumps generated in magnetic decorations that act as effective surface pinning centers (Bitter pinning [11]). In this way, several periodic Fe patterns of square symmetry with 50×50 dots were created at the surface of the single crystal. Large surface regions of

* Corresponding author. Tel.: +54-294-444-5171; fax: +54-294-444-5299.
E-mail address: hernan@cab.cnea.gov.ar (H. Pastoriza).
[1] Permanent address: Unitá INFM e Dipartimento di Fisica, Universitá di Roma Tre, Rome, Italy.

0038-1098/$ - see front matter © 2003 Elsevier Ltd. All rights reserved.
doi:10.1016/S0038-1098(03)00645-8

the sample were left free of Fe dots to detect the hexagonal pattern and to compare the induction field B inside and out of the Fe patterned region. The vortex structure was nucleated by cooling the sample in the presence of a magnetic field. The Fe pattern was chosen to make the area of its unit cell, a_{sq}^2, equal to that of the hexagonal vortex lattice induced by the applied field (one flux quantum per unit cell). The vortex lattice was visualized by magnetic decoration. The Fe structure from the magnetic decoration, as well as that of the periodic pattern, was observed at room temperature with a scanning electron microscope. When the Bitter and the periodic pattern coincide, the Fe clumps from the decoration were recognized by their irregular appearance as compared to the circular shape of the dots of the periodic pattern. The number of vortices per unit area in the patterned area was found to be the same as that in the non-patterned region (the same B).

Fig. 1 shows the vortex decoration on the Fe-patterned surface of a sample with $a_{sq} = 0.835$ μm, hereafter called top surface. The vortex structure corresponds to $B = 30.2$ G and the decoration was made at 4.1 K. The dark region marks the area where the square 2D pinning was generated. The square topology of the vortex structure induced by the periodic pattern is evident. The natural hexagonal symmetry of the solid is seen to be recovered outside the Fe patterned region in no more than two lattice parameters. The one to one site correspondence of Fe clumps from the decoration with the square pattern reveals that the 2D periodic pinning imposes the vortex liquid to solidify in a single crystal with square symmetry at the top surface.

To verify whether the sample is thick enough to allow the recovery of the hexagonal vortex symmetry, a magnetic decoration was made on the opposite surface of the Fe patterned one, hereafter called bottom surface. Fig. 2 shows the decoration at the bottom surface of a 4.5 μm thick sample, beneath the square Fe patterned region. The Delaunay triangulation of the vortex lattice is depicted. The picture shows that the hexagonal vortex lattice underneath the patterned area has one of its principal directions parallel to one of the square pinning potential axis. This shows that the presence of the square potential at the top surface breaks the rotational degeneracy of the hexagonal lattice nucleated in the sample region below the Fe pattern. The hexagons at the bottom of the sample make evident the coexistence of square and hexagonal symmetries along the vortex strings.

The results in Figs. 1 and 2 suggest the presence of a transition region between structures with equivalent energy:

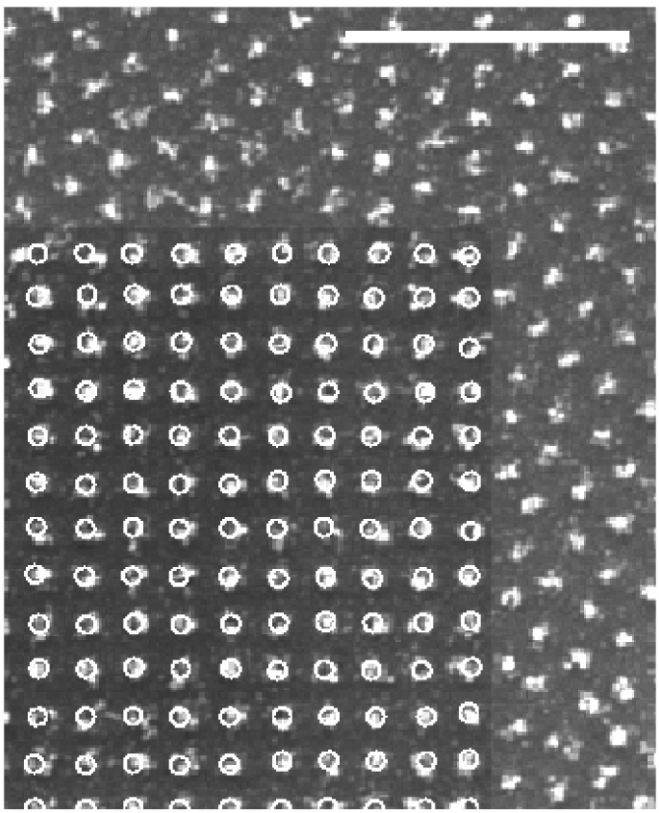

Fig. 1. Vortex decoration of the top surface of a sample with commensurate square magnetic pattern for a field of 30.2 G at 4.1 K. The Fe dots of the periodic structure are 260 nm in diameter and 60 nm in height. The dark area indicates the region where a periodic 2D square pattern was generated. The Fe dots positions are depicted with white circles. The scale bar corresponds to 5 μ m.

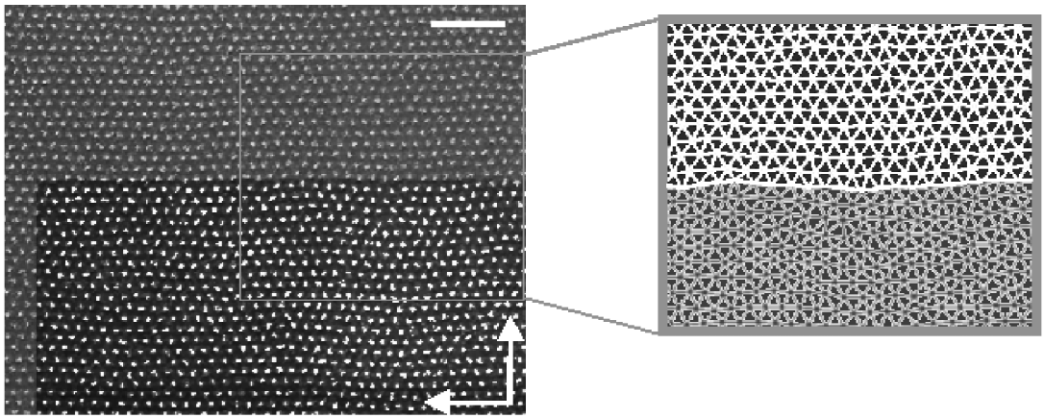

Fig. 2. Vortex decoration of the bottom surface of a 4.5 μm thick sample beneath the square Fe pattern indicated by the dark region with brighter spots. The insert depicts the corresponding Delaunay triangulation of the framed region, obtained joining the positions of next-near-neighbors vortices with straight lines. The picture shows that the hexagonal vortex lattice has one of its principal directions parallel to one of the square pinning potential axis (indicated by the arrows). The scale bar corresponds to 5 μm.

The square structure at one side of the wall, where the surface pinning potential compensates the increase of interaction energy corresponding to the square lattice, and the natural hexagonal symmetry of the vortex crystal at the other side.

To explore the change of the vortex topology along the sample thickness, we performed decorations of freshly cleaved bottom surfaces, analyzing the vortex structure below regions with square Fe patterns with the same a_{sq}. The cleaving method has the advantage of preparing excellent surfaces for decoration but does not allow us to choose a precise thickness. Repeating the cleaving process we were able to change the thickness of the original sample of 12.5 μm. Decoration of the bottom surface of samples with thickness, d, of 12.5, 5.75, 4.5, 3.5, 2.5 and 0.5 μm verified that the hexagonal symmetry was recovered at a distance between 3.5 and 4.5 μm.

The thinnest sample, with $d = 0.5$ μm, shows that the vortex structure has the square symmetry in the whole region beneath the Fe pattern, as depicted in Fig. 3. This result indicates that the engineered 2D pinning potential could be used to modify the melting or wetting conditions for the vortex system in a finite thickness close to the surface of the sample [12,13].

The magnetic decoration of vortices at the bottom surface of samples with different thicknesses allowed to locate the range of sample thickness where the change of vortex topology takes place and to investigate the internal microscopic structure of the interface. The interface region is detected close to the top surface and extends within the limits of 0.5 μm from that surface, where the structure is detected to remain square, and 4.5 μm where the topology is already found to be hexagonal. Thus, the hexagonal structure is recovered within a distance of at most 4 lattice parameters ($a \approx 1$ μm).

Despite the fact that the limits mentioned above are determined from decorations in thin samples, we will show that they can be taken as boundaries of the region where the topology transformation has to take place in a thick sample. It could be argued that in a thin sample the energy is minimized preserving the square symmetry (straight vortices). For a thick sample, the decrease in interaction energy induced by the symmetry change compensates the extra elastic energy from the increase of the vortex length. Therefore, the limit for the propagation of the square symmetry for a thick sample could be lower than that for a thin one. This is not the case, because the boundary condition requires the superconducting currents to flow parallel to the top surface of the sample in a distance of the order of the penetration length, λ. Thus, the vortices cannot change their direction at least within this distance; i.e. λ becomes the lower limit for the propagation of the square vortex structure independently of the thickness of the sample. As the field cooled vortex structure is frozen close to the melting temperature [11], $\lambda(T_m) \approx 0.4$ μm becomes the expected lowest limit for the propagation of the square vortex structure in thick samples.

Fig. 4 shows the decoration of the 3.5 μm thick sample underneath the square Fe patterned area shown in the previous figures. The picture corresponds to nearly half of the patterned area. Statistics made on hundreds of vortex unit cells below two different square Fe patterned regions indicate that from the total number of vortices in the interface 83%, belong to hexagonal deformed structures, while the rest are distributed in regions of square symmetry of few lattice parameters (15 vortices in average). About 85% of the deformed hexagons are distributed between two possible degenerate states rotated by 90 degrees. Each state is characterized by one lattice parameter equal in magnitude and parallel to one of the square Fe pattern, see Fig. 4. Remarkably, we had found that the relative abundance (within 3%) of distorted hexagonal and square symmetry

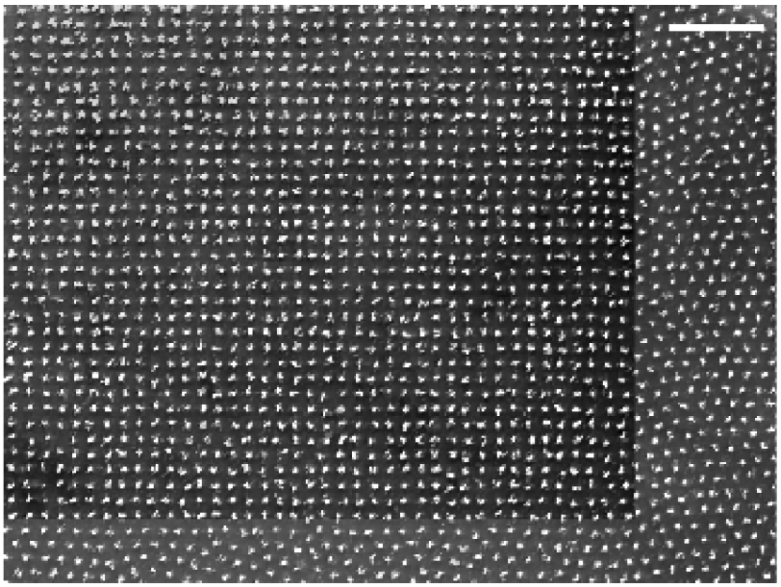

Fig. 3. Vortex decoration of the bottom surface of the thinnest sample investigated, $d = 0.5$ μm. It shows a complete square symmetry of the whole vortex structure beneath the periodic 2D square pattern in the top surface (dark area). The scale bar corresponds to 5 μm.

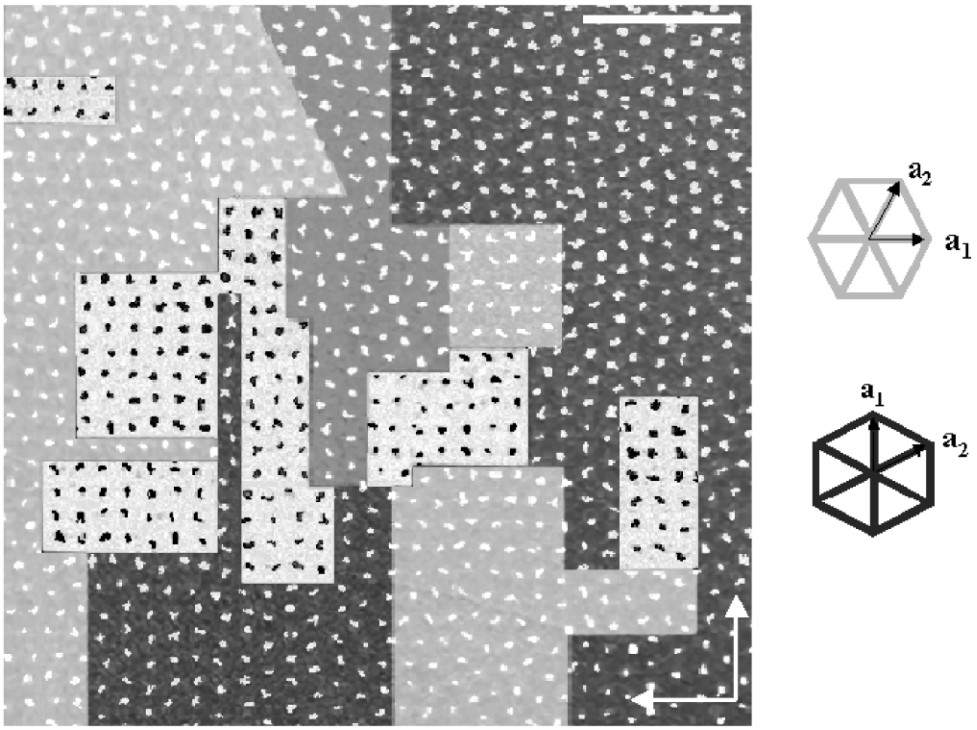

Fig. 4. Image of the vortex topology in the interface. Decoration of the bottom surface of the 3.5 μm thick sample underneath the square Fe patterned area, see text. Arrows indicate the principal directions of the square pattern on the top surface. Three distorted hexagonal symmetries coexisting with fourfold symmetry regions are observed. Black clumps: domains of vortices in square symmetry matching the square Fe pattern at the top surface. White clumps correspond to domains of vortices with distorted hexagonal symmetry underneath the square Fe patterned area. The unit cell area of these hexagons is equal to the square pattern unit area. Light and dark gray background: Vortices in distorted hexagons with one of the unit vectors parallel and equal to one of those of the square pattern. Gray background: Vortices in distorted hexagons rotated 15 degrees with respect to the horizontal principal direction of the square pattern. The scale bar corresponds to 5 μm.

regions is the same at the bottom of 2.5 and 3.5 μm thick samples, underneath two identical Fe patterned regions. If the decorated structure at the bottom surface were to be sample thickness dependent, we would expect that a thinner sample should show a larger concentration of square domains at expenses of a decrease of the hexagonal ones, contrary to the experimental finding. The fact that the proportions of deformed hexagonal and square symmetry regions do not change significantly between the 2.5 and 3.5 μm thick samples is indicative of a quite robust interface extending for more than 1 μm. From the previous results we conclude that the configuration shown in Fig. 4 quite likely represents not only the mixture of symmetries that takes place when transforming from square to hexagonal in thin samples, but also that in thick samples.

It is important to remark that each decoration implies a realization of a new experiment, including cleaving the sample to adjust its thickness. The thickness independence of the proportion between square and distorted hexagonal domains does not imply their site reproduction in different experiments under the same square Fe pattern, see Fig. 5. This result and the observed change in relative abundance between the two hexagonal degenerate states are consistent with the statistical reproduction of equivalent experimental realizations in homogeneous samples.

Another characteristic of the interface is that the area of both, the hexagonal distorted as well as the square unit cell at the bottom of the 3.5 and 2.5 μm samples coincides within 2% with that of the square and hexagonal crystals at each side of the interface in the thick sample limit. This strongly supports that the transformation from the square to the hexagonal symmetry is made under the condition of constant unit cell area (uniform B) across the interface. From the results, the transformation from the described mixture of phases within the interface region to the uniform hexagonal and square symmetries has to take place within one and two micrometers, respectively (one and two lattice parameters). We have not observed these transformations because the cleaving technique does not permit to choose a thickness of the sample with the necessary precision.

Recent computer simulations [14] describing the vortex interaction with a 2D infinite pinning potential have reproduced much of the structure detected in our samples of finite thickness. Mixture of symmetries as the one we observe at the interface were obtained in the simulations as metastable states under quenching conditions. The stabilization of this state could in principle be due to the presence of weak bulk pinning, not considered in the simulations. However, the stability of the fixed proportion of square and deformed hexagonal structures observed in samples of different thicknesses has not been made explicit in Ref. [14]. It might represent the intrinsic interface interconnecting 3D

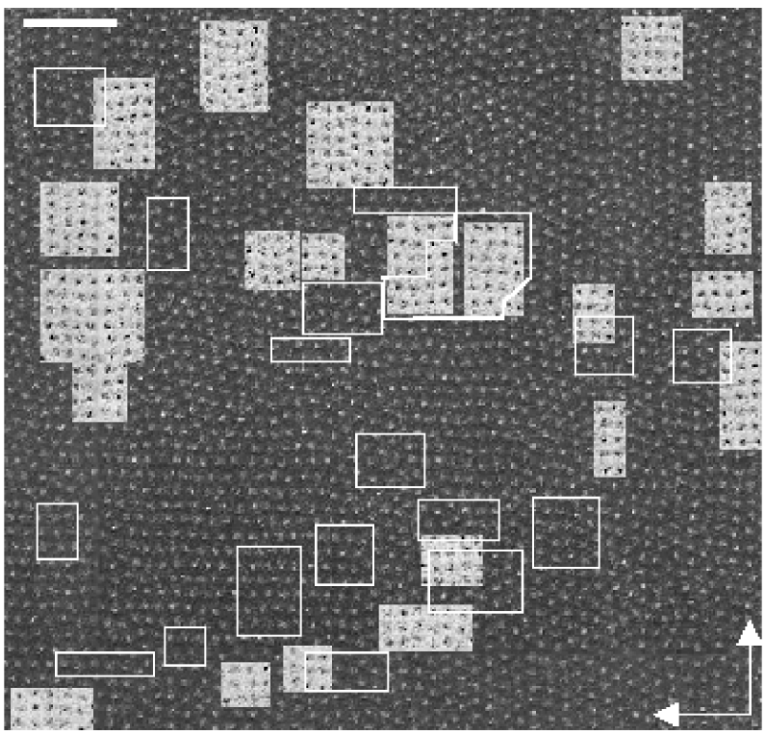

Fig. 5. Comparison of vortex interface structures at 3.5 and 2.5 μm underneath the same square Fe pattern. The picture is that of the 3.5 μm sample where the black clumps areas depict the square symmetry regions and the superimposed white frames indicate the location of the square symmetry regions in the 2.5 μm thick sample. The image shows the vortex lattice in the region underneath the whole patterned area and the scale bar corresponds to 5 μm.

square structures with the 3D hexagonal lattice at constant B or the consequence of the presence of bulk pinning in real systems, stabilizing thickness independent metastable states at the freezing temperature. Further experimental and theoretical work is necessary to clarify this point.

In conclusion, the combination of electron-beam lithography and magnetic decoration techniques have allowed to demonstrate that the vortex liquid can be solidified in two coexisting crystals with different symmetries along the vortex length. The square vortex line lattice induced by the engineered 2D Fe pattern at one end of the vortex strings is shown to propagate in thin samples up to a distance of the order of a micrometer, making the transition towards the hexagonal lattice through an interface. The 3D nature of the induced square lattice and the thickness independence of the proportions of square and deformed hexagonal structures at the interface, strongly support that the symmetry transformation in thick samples takes place very close to the Fe patterned surface through the same mixture of structures. The continuous nature of the vortex strings is the unique property that allows us to visualize the transformation of the structure along the vortex direction in a transition width of the order of the average separation between vortices. The experimental data provide valuable information to stimulate and verify the results of theoretical modeling of interfaces.

Acknowledgements

We acknowledge A.A. Aligia, J. Lorenzana, C. Balseiro, E. Jagla, P. Cornaglia and F. Laguna for valuable discussions and E. Martínez for careful reading of the manuscript. This work was partially supported by Agencia Nacional de Promoción Científica y Tecnológica, by Fundación Antorchas and by Consejo Nacional de Investigaciones Científicas y Técnicas, Argentina.

References

[1] L.D. Landau, E.M. Lifshitz, Statistical Physics, third ed., Pergamon, Oxford, 1993.
[2] P.M. Chaikin, T.C. Lubensky, Principles of Condensed Matter Physics, first ed., Cambridge University Press, Cambridge, 1995.
[3] H. Safar, P.L. Gammel, D.A. Huse, D.J. Bishop, J.P. Rice, D.M. Ginsberg, Phys. Rev. Lett. 69 (1992) 824.
[4] H. Pastoriza, M.F. Goffman, A. Arribére, F. de la Cruz, Phys. Rev. Lett. 72 (1994) 2951.
[5] E. Zeldov, et al., Nature 375 (1995) 373.
[6] D.R. Nelson, V.M. Vinokur, Phys. Rev. B 48 (1993) 13060.
[7] S.A. Grigera, E. Morre, E. Osquiguil, C. Balseiro, G. Nieva, F. de la Cruz, Phys. Rev. Lett. 81 (1998) 2348.
[8] G. Blatter, et al., Rev. Mod. Phys. 66 (1994) 1125.
[9] D.S. Fisher, M.P.A. Fisher, D.H. Huse, Phys. Rev. B 43 (1991) 130.
[10] T. Giamarchi, P. Le Doussal, Phys. Rev. B 52 (1995) 1242.
[11] Y. Fasano, J.A. Herbsommer, F. de la Cruz, F. Pardo, P.L. Gammel, E. Bucher, D.J. Bishop, Phys. Rev. B 60 (1999) R15047. Y. Fasano, M. Menghini, F. de la Cruz, G. Nieva, Phys. Rev. B 62 (2000) 15183.
[12] T. Joseph, Ch. Dasgupta, cond-mat/0210153.
[13] S.S. Banerjee, By means of differential-magneto-optics the order as well as the temperature of the melting transition were found to be the same for patterned and non-patterned regions within the present temperature sensitivity of the technique (private communication).
[14] P. Cornaglia, M.F. Laguna, Phys. Rev. B. 67 (2003) 132503.